Antisymmetric resonant mode and negative refraction in double-ring resonators under normal-to-plane incidence

P. Ding,[1,2] E. J. Liang,[1,*] L. Zhang,[1] Q. Zhou,[1] and Y. X. Yuan[1]

[1]*School of Physical Science and Engineering and Key Laboratory of Materials Physics of Ministry of Education of China, Zhengzhou University, Zhengzhou 450052, China*

[2]*Department of Mathematics and Physics, Zhengzhou Institute of Aeronautical Industry Management, Zhengzhou 450015, China*

(Received 19 July 2008; published 13 January 2009)

Compared to metallic composite metamaterials of double split-ring resonators with wires, double-ring resonators without additional wires are simple to engineer. In this paper, we have numerically studied the transmittance of double split- and closed-ring resonators at normal-to-plane incidence and identified their fundamental resonance modes. It is found that the antisymmetric and symmetric resonance modes originate from the out-of-phase and in-phase oscillations of surface charges in the neighboring legs of the double-ring resonators, respectively. The coupling of the antiparallel induced currents in the neighboring legs gives rise to magnetic resonance and consequently negative permeability of the antisymmetric mode. The negative refraction transmission of the double-ring resonators at normal-to-plane incidence is verified by dispersion curve and wedge-shaped model simulations. Our study provides a route to negative refraction metamaterial design by using the antisymmetric resonance mode of the simple double-ring structure at normal-to-plane incidence which is of particular importance for the terahertz and infrared domain.

DOI: 10.1103/PhysRevE.79.016604 PACS number(s): 41.20.Jb, 42.70.Qs, 78.20.Ci, 73.20.Mf

I. INTRODUCTION

Metallic double split-ring resonators (DSRRs), the most well-known magnetic metamaterial model, have gained much attention since the seminal proposal by Pendry [1]. The magnetic resonance of the DSRRs and their variations is generally formulated by an *LC* circuit since the induced circulating currents in the rings contribute to the inductance *L* and the splits account for the capacitance *C* [1–6]. The inner ring tunes the resonance to lower frequencies by increasing the gap capacitance of the outer ring. The electric response of split-ring resonators is described by the negative permittivity of an effective medium, which is usually excited at higher frequencies and does not overlap with the region of negative permeability [7]. Therefore, a negative index was generally realized by combining thin metallic wires with metallic DSRRs, in which the wires and the DSRRs were responsible for the negative permittivity and the negative permeability, respectively [2,8]. When a desired magnetic resonance is expected, the polarization dependence of the incident electromagnetic waves must be considered due to the highly electromagnetic anisotropy of the DSRRs [9–11]. An incident wave propagating parallel to the ring plane was usually used to achieve negative permeability [2,8].

Recently, it was reported that a negative index of refraction (NIR) could be achieved with either double split-ring (DSR) or double closed-ring (DCR) resonators at parallel incidence, without the assistance of metallic wires [12,13]. These simple structures are very attractive for their simplicity in fabrication. In particular, the antisymmetric resonance modes associated with the antiparallel induced currents in the neighboring edges of concentric double rings were suggested to contribute to the negative effective permeability [12,13]. The antisymmetric resonance mode can also be excited in DSRR metamaterials when the light propagates perpendicular to the ring plane [14]. However, the possibility of achieving negative refraction by using the antisymmetric resonant modes excited at normal-to-plane incidence has not been explored.

In this paper, we study the electromagnetic response of DCR and DSR resonators at normal-to-plane incidence. Based on investigation of resonance transmission, near-field patterns, and surface current distributions, we obtain a comprehensive and consistent picture of the resonance mode in double-ring metamaterials with different geometrical configurations. The contribution of the antisymmetric resonant mode to negative refraction is underlined and negative refraction transmission is verified.

II. STRUCTURES AND SIMULATION METHOD

The geometry of the DCR resonator is chosen identically with that of Ref. [12] for comparison, as shown in Fig. 1(a). The unit cell of the structure has dimensions of $a=3.8$ mm in the ring plane and $b=2.5$ mm in the perpendicular direction. The square copper ring has a thickness of 0.02 mm. The geometric parameters l and w are selected to be 3.0 and 0.2 mm, respectively. The spacing g between the inner and outer rings is 0.1 mm. The rings are designed onto a 0.25-mm-thick Teflon substrate with relative dielectric constant of 2.1. The DSR resonator has split width of $g=0.1$ mm in both rings.

The numerical simulations were performed by using the finite-element method (Ansoft's HFSS), whose accuracy has been confirmed by the good agreement between the numerical and the experimental results [15,16]. A theoretical model based on an artificial waveguide with two ideal magnetic conductor and two ideal electric conductor planes as the transverse boundaries was employed, which is equivalent to

*ejliang@zzu.edu.cn

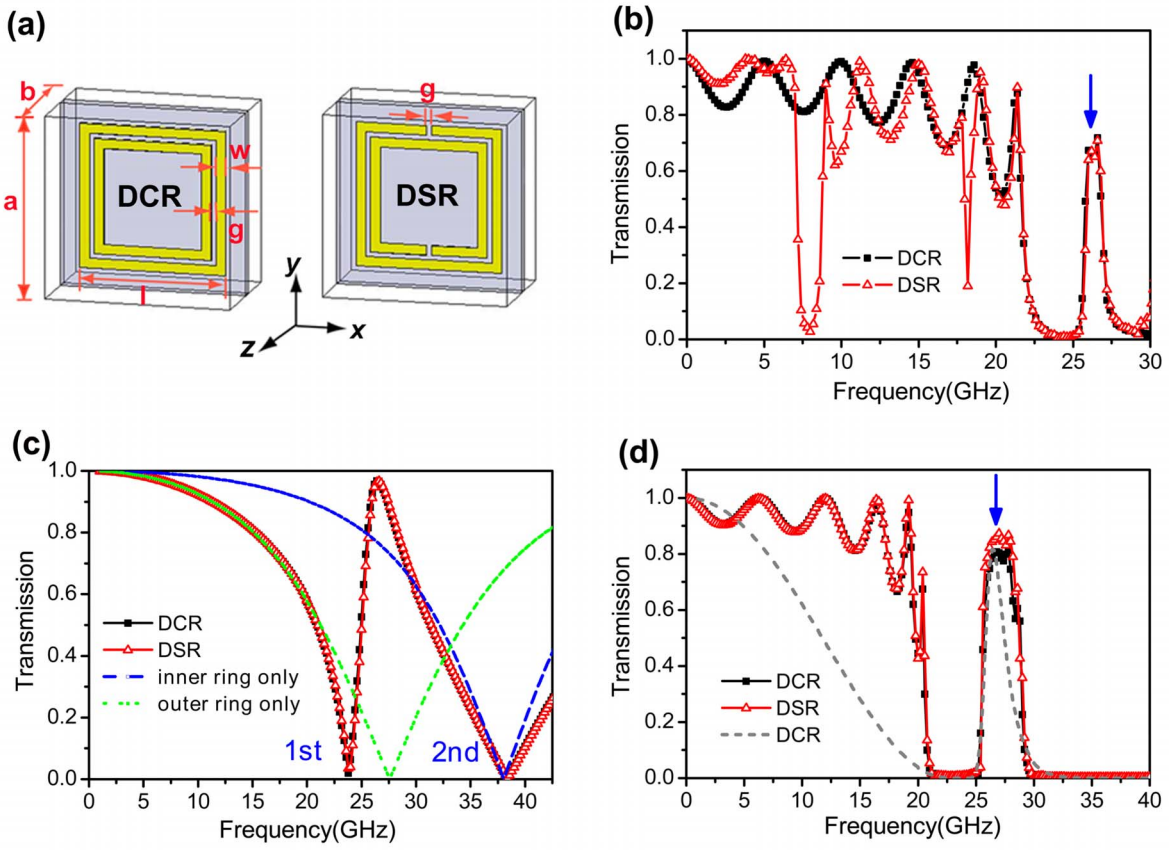

FIG. 1. (Color online) (a) Unit cells of the metallic double closed-ring (DCR) and double split-ring (DSR) resonators. (b) Transmission coefficients for both resonators with six units closely stacked in the wave propagation direction at in-plane incidence. (c) Transmission coefficients of the outer ring, inner ring, DCR, and DSR resonators at normal-to-plane incidence. (d) Transmission coefficients of the DCR and DSR resonators with six units closely stacked in the wave propagation direction at normal-to-plane incidence. The dotted line is the transmission coefficient of a single DCR resonator involved six times, which equals a wave transmitting though six independent DCR resonators.

an infinite layer medium illuminated by a normally incident plane wave [17,18]. In our calculation, a polarized incident wave with its electric component perpendicular to the split-bearing side of the ring is adopted for the sake of eliminating the undesired bianisotropic effect via asymmetry [9].

III. SIMULATION RESULTS AND DISCUSSION

A. Transmission spectra for parallel and normal incidence

In order to reveal the difference between the electromagnetic responses excited at normal and parallel incidence, we first give the transmission results for the DCR and DSR resonators at parallel incidence with the electric field polarized along the *y* axis in Fig. 1(b). Here, one unit cell in the transverse plane and six unit cells in the electromagnetic propagation direction are used. The transmission dips at about 8 and 18 GHz for the DSR structure corresponding to the magnetic resonances (*LC* resonance) of the outer and inner rings, respectively [19], while the transmission peak at about 26 GHz for both DCR and DSR resonators was identified as the passband with negative index of refraction [12,13].

Next we focus on the electromagnetic response of the DCR and DSR resonators at normal-to-plane incidence with the electric field polarized along the *y* axis and the magnetic field along the *x* axis. In this configuration, only electric resonance is excited and the magnetic resonance originating from the magnetic component of the incident light or from the electric-magnetic coupling is eliminated. Figure 1(c) shows the transmission spectra of the DCR and DSR resonators as well as those of outer and inner rings alone. The outer and inner rings alone give rise to resonance frequencies at about 27 and 38 GHz, respectively. From a plasmonic point of view, the electric resonances are associated with the surface charge oscillating along the non-split-bearing legs driven by the external electric field. The DCR and DSR resonators exhibit identical transmission spectra in the chosen spectral domain because a small geometrical discrepancy between DSR and DCR (i.e., the splits existing on the legs perpendicular to the electric field) is expected to have little influence on the electric response. Two resonances appear at about 24 and 38 GHz. The shifts of the two modes relative to those of the outer and inner rings alone result from the coupling of the outer and inner rings. A passband is formed between the two electric resonances.

Figure 1(d) shows the transmission spectra with six unit cells stacked along the wave propagation direction. It is noticed that the transmission coefficients of the transmission

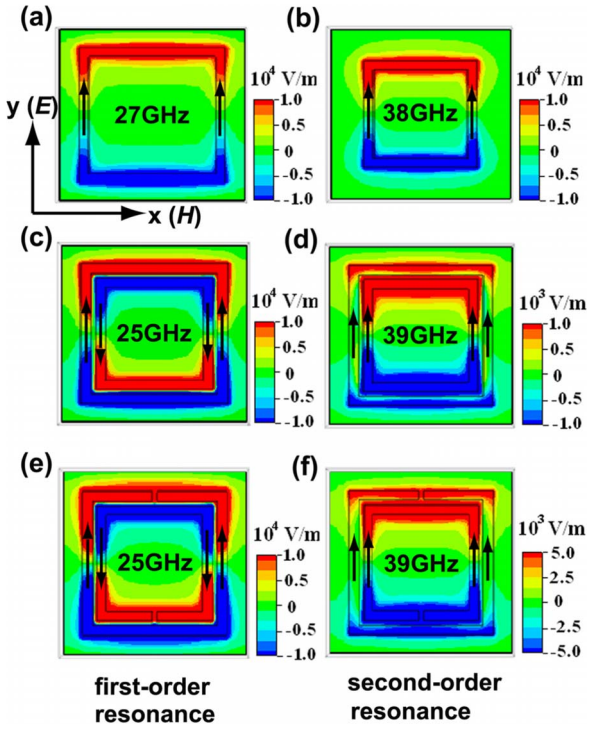

FIG. 2. (Color online) Amplitudes of the electric field component E_z in the x-y plane 80 μm above the structure for the outer (a) and inner (b) rings alone, and the DCR (c),(d) and DSR (e),(f) resonators. The arrows indicate the directions of the induced surface currents.

band from 25 to 30 GHz and its bandwidth at normal-to-plane incidence are larger than those at parallel incidence [Figs. 1(b) and 1(d)]. In addition, it becomes more rectangular with respect to that with six independent unit cells as shown by the dotted line of Fig. 1(d). This suggests that there exists coupling among the cells in addition to that of the outer and inner rings.

B. Antisymmetric and symmetric resonance modes excited at normal incidence

In order to get an insight into the physical picture of both resonances indicated in Fig. 1(c), we calculated the induced currents for the outer and inner rings alone as well as the DCR and DSR resonators and the E_z distribution in the near field 80 μm above the structure as shown in Fig. 2. For clarity, the directions of the currents are indicated by arrows. It is shown that the double-ring resonators present not only the relative shifts of resonant frequency but also the new coupled mode pairs, by comparing both the resonant frequencies and the electric field distributions of the DCR and DSR resonators with those of the outer or inner ring alone [Figs. 1(c) and 2(a)–2(f)]. Figures 2(c)–2(f) indicate that the first- and second-order resonance modes originate from the out-of-phase and in-phase surface charge oscillations in the neighboring legs along the y axis of the double rings, respectively. They are identified as the antisymmetric and the symmetric mode, respectively, in analogy to the plasmon modes of double split-ring resonators excited in the visible regime [14]. It is also shown that the splits with small gap have negligible influence on the E_z field pattern or surface current distribution. This is consistent with the transmission spectra calculations discussed above.

C. The dependence of antisymmetric resonance modes on geometrical parameters

The antisymmetric and symmetric resonance modes in the DCR and DSR resonators at normal incidence result from the antisymmetric and symmetric coupling of the electric resonances of the outer and inner rings. In order to see the coupling more clearly, we studied the dependence of the antisymmetric mode on the geometric parameters, i.e., the spacing between the inner and the outer rings. Since the coupling becomes weaker with larger spacing, the antisymmetric resonance mode shifts to higher frequencies and approaches the resonance frequency of the outer ring alone with increasing spacing, as shown in Fig. 3(a).

Figures 3(b) and 3(c) show the magnetic field maps in the x-y plane for 0.2 and 0.5 mm spacing between the outer and inner rings, respectively. It is shown that the magnetic field is localized in the area between the inner and outer rings for $g=0.2$ mm but not for $g=0.5$ mm. This also suggests a weaker coupling for larger spacing between the outer and inner rings.

Furthermore, the resonance coupling between the neighboring metallic legs also depends greatly on the dielectric property of the surrounding material. The frequency of the antisymmetric mode can be tailored obviously by changing the dielectric function of the surrounding material as shown in Fig. 3(d). However, the magnetic fields in the spacing area cancel each other for the symmetric mode because the induced currents in the neighboring legs are parallel. Therefore, a slight dependence of the symmetric mode on the dielectric function of the surrounding material is expected.

Although Figs. 1 and 2 show identical electrical resonance for DCR and DSR resonators, larger split width or more splits have obvious effects on the resonance frequencies as shown in Figs. 4(a) and 4(b). It is found that both the antisymmetric and the symmetric modes shift to higher frequencies for larger splits.

D. The contribution of the antisymmetric mode to negative refraction

The external electric field excites cut-wire-type electric resonance in both outer and inner rings and the interaction of the outer and inner rings gives rise to coupled antisymmetric and symmetric resonance mode pairs. Negative permittivity can be achieved by the intrinsical electric resonance. However, negative refraction requires also a negative permeability at the same frequency range, which may be obtained if the resonant magnetic response of the DCR or DSR resonator to the magnetic field resulting from the induced currents in the neighboring legs of the outer and inner rings is sufficiently strong. Magnetic resonance for the symmetric mode is not expected since the currents in the four legs are all parallel and hence their magnetic fields cancel each other over the whole area of the structure. In Fig. 5 we show the

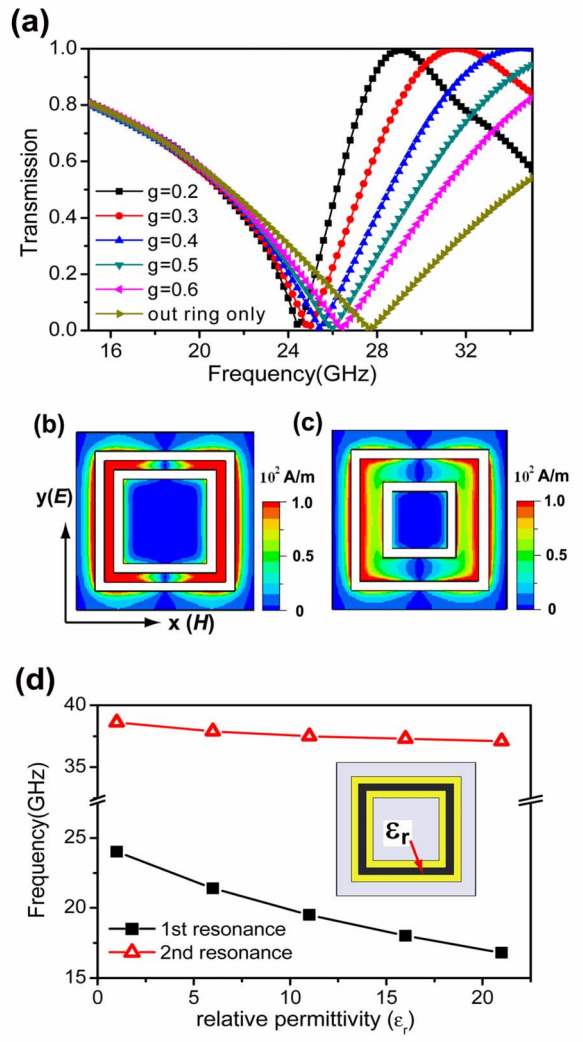

FIG. 3. (Color online) (a) Dependence of transmission coefficients on the spacing g between the neighboring legs of the outer and inner rings. (b),(c) Amplitudes of the magnetic field component H_z in the x-y plane for $g=0.2$ mm (at 25 GHz) and $g=0.5$ mm (at 27 GHz), respectively. (d) Dependence of the first- and second-order resonance frequencies on the dielectric function of the surrounding material between the legs with $g=0.1$ mm.

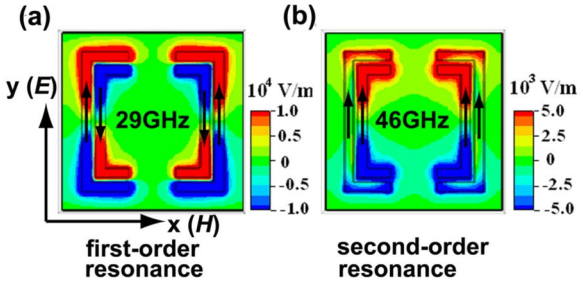

FIG. 4. (Color online) Amplitudes of the electric field component E_z in the x-y plane 80 μm above the structure at the first-order (a) and the second-order (b) resonance frequencies. The directions of the induced surface current are indicated by black arrows.

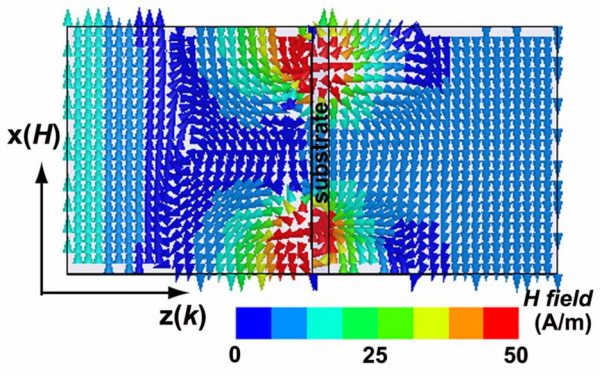

FIG. 5. (Color online) Magnetic field map for the DCR resonator at 25.2 GHz in the x-z plane with y coordinate in the midpoint of the ring edge.

magnetic field distribution of the DCR resonator in the x-z plane for the antisymmetric mode. Both Fig. 3(b) and Fig. 5 indicate that the magnetic response of the DCR resonator is strong for the antisymmetric mode. It is therefore possible to achieve negative permeability and consequently negative refraction with this mode.

E. The verification of a negative index of refraction

To verify resonance transmission with negative index, the retrieval procedures [20,21] are generally used to obtain the effective medium parameters of simultaneous negative permittivity and permeability. However, the retrieved results are questionable when the unit cell of the proposed structure is comparable in size with the incident wavelength of the resonant frequency. The unit cell discussed here has the electric size of about 1/3 in the transverse direction (in the x-y plane) and above 1/5 in the wave propagation direction (along the z axis) with regard to the free space wavelength of 26 GHz. Therefore, we demonstrate the negative refraction behaviors of the double-ring resonators at normal-to-plane incidence by calculating the dispersion diagram and simulating the refraction through a wedge-shaped prism, both of which provide significant physical insights into the nature of the artificial material and give unambiguous evidence of negative refraction [22–24].

The finite-element eigenmode solver with periodic boundary conditions is used to calculate the dispersion diagram of DCR resonators under normal-to-plane incidence with electric field along the y axis and magnetic field along the x axis [24]. The resulting dispersion curves shown as the frequency versus the phase advance across a unit cell are given in Fig. 6. For comparison, the dispersion curve of a single ring structure (i.e., the outer and inner rings are united by filling the gap with metal) is also calculated as shown by the light gray line with triangles. There are three branches of propagating modes within the spectral domain of interest for the DCR resonator. The second propagating mode appearing around 25.2 GHz with a bandwidth of 0.45 GHz (red lines with circles in Fig. 6) presents clearly a negative slope, which suggests that the phase and group velocity have opposite signs and the medium supports backward-wave propaga-

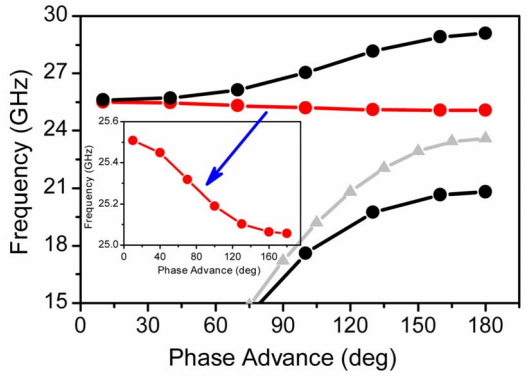

FIG. 6. (Color online) Dispersion curves [black or red (gray) line with circles] for the DCR resonators at normal-to-plane incidence with the electric field polarized along the y axis. The second branch [red (gray) line with circles] corresponds to the left-handed passband. The inset shows a magnified plot. The light gray line with triangles represents the dispersion of a single-ring structure (i.e., the outer and inner rings in the DCR are united by filling the gap with metal).

tion. Associated with the backward propagation property, media with negative parameters should be characterized by a negative refractive index [25].The dispersion diagram also suggests that the transmission band from about 25 to 30 GHz, shown in Fig. 1(c), is actually comprised of a left-handed and a right-handed band.

A refraction simulation with a wedge-shaped model positioned between two magnetically conducting plates with the absorber boundary conditions at the side faces is performed (more details about the simulation conditions can be found in [12,26]). For the wedge model, eight unit cells are arrayed along the y axis and seven unit cells along the z axis. The refraction interface has a staircase pattern with one-unit-cell step on the y axis and the z axis, which can be referred to as a wedge of 33.3°. Figure 7 shows the typical magnetic field distribution at the frequency of 25.2 GHz, which demonstrates unambiguously a negative refraction of the DCR resonator at normal-to-plane incidence. This confirms the negative index propagation mode revealed by the dispersion diagram. A similar negative refraction for the DSR resonator is also demonstrated (not shown here).

Finally, we wish to point out that a negative slope of the phase advance versus frequency can be taken as indubitable proof of a NIR medium for a propagating mode but not for a complex mode. For a complex mode in a shielded dielectric image guide, the phase constant of the complex mode also decreases with the frequency in a small frequency range in a non-NIR medium as shown by Strube and Arndt [27], but the total power transmitted by the complex wave through the

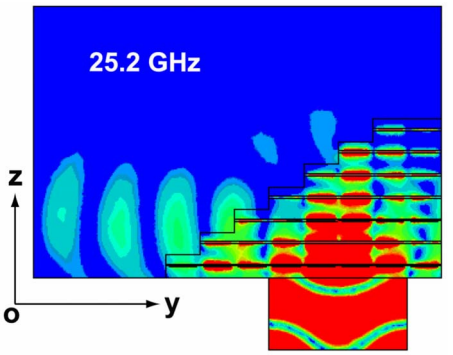

FIG. 7. (Color online) Magnitude distributions of the magnetic field in the y-z plane with $x=\pm 1.25$ mm for the wedge-shaped negative refraction of DCR resonators at 25.2 GHz.

total cross section of the shielded dielectric image guide is zero. For a propagating mode, the NIR nature is characterized by the opposite sign of the phase velocity and the group velocity with unambiguous transmission power (see Figs. 1 and 7).

IV. CONCLUSION

In summary, we verified the negative index transmittance of DCR and DSR resonators at normal incidence. The antisymmetric resonance mode excited in a DCR or DSR resonator is described and a mechanism for obtaining NIR is revealed that is different from the common view of a geometric LC resonance. The intrinsic particle-plasmon resonance provides the negative permittivity, while the induced antisymmetric mode due to the resonance coupling is responsible for the negative permeability. Resonance transmissions with negative index are further confirmed by the dispersion diagram and the wedge-shaped model. Unlike the conventional designs based on metal-dielectric-metal composites (for instance, SRRs with wires or the so-called fishnet structure [28]), a double-ring resonator metamaterial with metallic patterns printed on one side of the substrate reduces the complicity of fabrication. Although we have identified the negative refraction using the electric-induced antisymmetric mode only within the microwave domain, it is possible to extend the DCR and DSR resonator metamaterials to the terahertz or ir domain where the normal-to-plane incidence is of top priority.

ACKNOWLEDGMENTS

This work was supported by the Natural Science Foundation of the Education Department of Henan Province of China (Grant No. 2008A140012). We acknowledge Dr. Q. Z. Xue from the Institute of Electronics, Chinese Academy of Sciences, for his support.

[1] J. P. Pendry, A. J. Holden, D. J. Robbins, and W. J. Stewart, IEEE Trans. Microwave Theory Tech. **47**, 2075 (1999).
[2] D. R. Smith, W. J. Padilla, D. C. Vier, S. C. Nemat-Nasser, and S. Schultz, Phys. Rev. Lett. **84**, 4184 (2000).
[3] K. Aydin, I. Bulu, K. Guven, M. Kafesaki, C. M. Soukoulis, and E. Ozbay, New J. Phys. **7**, 168 (2005).
[4] C. Enkrich, F. Pérez-Willard, D. Gerthsen, J. F. Zhou, T. Koschny, C. M. Soukoulis, M. Wegener, and S. Linden, Adv. Mater. (Weinheim, Ger.) **17**, 2547 (2005).
[5] H. Chen, L. Ran, J. Huangfu, X. Zhang, K. Chen, T. M. Grzegorczyk, and J. A. Kong, Phys. Rev. E **70**, 057605 (2004).
[6] G. Dolling, C. Enkrich, M. Wegener, J. F. Zhou, C. M. Soukoulis, and S. Linden, Opt. Lett. **30**, 3198 (2005).
[7] T. Koschny, M. Kafesaki, E. N. Economou, and C. M. Soukoulis, Phys. Rev. Lett. **93**, 107402 (2004).
[8] R. A. Shelby, D. R. Smith, and S. Schultz, Science **292**, 77 (2001).
[9] R. Marqués, F. Medina, and R. Rafii-El-Idrissi, Phys. Rev. B **65**, 144440 (2002).
[10] N. Katsarakis, T. Koschny, M. Kafesaki, E. N. Economou, and C. M. Soukoulis, Appl. Phys. Lett. **84**, 2943 (2004).
[11] N. Katsarakis, G. Konstantinidis, A. Kostopoulos, R. S. Penciu, T. F. Gundogdu, M. Kafesaki, E. N. Economou, T. Koschny, and C. M. Soukoulis, Opt. Lett. **30**, 1348 (2005).
[12] Z. G. Dong, M. X. Xu, S. Y. Lei, H. Liu, T. Li, F. M. Wang, and S. N. Zhu, Appl. Phys. Lett. **92**, 064101 (2008).
[13] Z. G. Dong, S. Y. Lei, M. X. Xu, H. Liu, T. Li, F. M. Wang, and S. N. Zhu, Phys. Rev. E **77**, 056609 (2008).
[14] H. Guo, N. Liu, L. Fu, T. P. Meyrath, T. Zentgraf, H. Schweizer, and H. Giessen, Opt. Express **15**, 12095 (2007).
[15] T. J. Yen, W. J. Padilla, N. Fang, D. C. Vier, D. R. Smith, J. B. Pendry, D. N. Basov, and X. Zhang, Science **303**, 1494 (2004).
[16] H. T. Chen, W. J. Padilla, J. M. O. Zide, A. C. Gossard, A. J. Taylor, and R. D. Averitt, Nature (London) **444**, 597 (2006).
[17] M. Beruete, M. Sorolla, and I. Campillo, Opt. Express **14**, 5445 (2006).
[18] M. Beruete, I. Campillo, M. Navarro-Cia, F. Falcone, and M. S. Ayza, IEEE Trans. Antennas Propag. **55**, 1514 (2007).
[19] M. Kafesaki, T. Koschny, R. S. Penciu, T. F. Gundogdu, E. N. Economou, and C. M. Soukoulis, J. Opt. A, Pure Appl. Opt. **7**, S12 (2005).
[20] D. R. Smith, D. C. Vier, T. Koschny, and C. M. Soukoulis, Phys. Rev. E **71**, 036617 (2005).
[21] X. Chen, T. M. Grzegorczyk, B. I. Wu, J. Pacheco, Jr., and J. A. Kong, Phys. Rev. E **70**, 016608 (2004).
[22] J. Valentine, S. Zhang, T. Zentgraf, E. Ulin-Avila, D. A. Genov, G. Bartal, and X. Zhang, Nature (London) **455**, 376 (2008).
[23] D. R. Smith, Willie J. Padilla, D. C. Vier, S. C. Nemat-Nasser, and S. Schultz, Phys. Rev. Lett. **84**, 4184 (2000).
[24] D. R. Smith and J. B. Pendry, J. Opt. Soc. Am. B **23**, 391 (2006).
[25] V. G. Veselago, Sov. Phys. Usp. **47**, 509 (1968).
[26] Z. G. Dong, S. N. Zhu, H. Liu, J. Zhu, and W. Cao, Phys. Rev. E **72**, 016607 (2005).
[27] J. Strube and F. Arndt, IEEE Trans. Microwave Theory Tech. **33**, 391 (1985).
[28] M. Kafesaki, I. Tsiapa, N. Katsarakis, T. Koschny, C. M. Soukoulis, and E. N. Economou, Phys. Rev. B **75**, 235114 (2007).